The International Journal of Advanced Manufacturing Technology (2019) 100:2333–2348
https://doi.org/10.1007/s00170-018-2793-0

ORIGINAL ARTICLE

The selection of temperature-sensitivity points based on K-harmonic means clustering and thermal positioning error modeling of machine tools

Yang Li[1] · Ji Zhao[1] · Shijun Ji[1] · Fusheng Liang[1]

Received: 29 January 2018 / Accepted: 28 September 2018 / Published online: 16 October 2018

Abstract
In the thermal error compensation technology of CNC machine tools, the core is to establish a mathematical model of thermal error with high predictive accuracy and strong robustness. The prerequisite for the error model is to select the optimum temperature-sensitivity points, which can inhibit the multi-collinearity problem among temperature points and improve the predictive accuracy and robustness of the error model. In this paper, K-harmonic means (KHM) clustering is introduced for the first time to select the temperature-sensitivity points in the field of error modeling. In statistical numerical experiments, it is verified that KHM clustering is very stable and requires relatively small number of iterations to converge comparing with the common clustering methods such as K-means (KM) clustering and fuzzy C-means clustering (FCM). Then, the effect of KHM clustering on the selection of temperature-sensitivity points is validated in the actual experiments. Multiple linear regression model combined with KHM clustering (MLR-KHM) is adopted to construct the thermal error model of positioning error. The experimental results demonstrate that the predictive accuracy and robustness of MLR-KHM error model can conform with the requirements of the error compensation.

Keywords CNC machine tools · Thermal error · Temperature-sensitivity point selection · K-harmonic means clustering

1 Introduction

With the widespread application and rapid development of precision and ultra-precision manufacturing technology, the requirement for processing precision of computer numerical control (CNC) machine tools is increasing. However, due to the thermal deformation of the machine tool structure during operation, relative position between the cutter and the workpiece changes, which eventually leads to the machining errors. Thermally induced errors account for approximately 40–70% of the total errors of a machine tool [1]. Therefore, thermal errors must be minimized.

The common methods to reduce the thermal errors are error avoidance and error compensation [2, 3]. The error avoidance method controls thermal errors in the design and construction phases of machine tools, which is a hardware compensation. Although this method can improve the accuracy of machine tools, the costs will dramatically increase. On the contrary, the error compensation method is a cost-efficient way, which creates an artificial error to offset the original thermal error. This is a software compensation, which is combined with hardware compensation in practice application.

An accurate thermal error model is the prerequisite of error compensation. At present, theoretical modeling and empirical modeling are two prevailing modeling methods.

In theoretical modeling, through the calculations of heat generations and convective heat transfer coefficients of different components in a machine tool, the temperature distribution can be obtained, and the deformation can be also gained [4–7]. While, the formula of heat transfer is a differential equation which is too complicated to be solved, and the inexact boundary conditions lead to inaccurate results in the actual situation. Theoretical modeling aids to understand the heat transfer

Electronic supplementary material The online version of this article (https://doi.org/10.1007/s00170-018-2793-0) contains supplementary material, which is available to authorized users.

✉ Fusheng Liang
ldsheng1332@163.com

[1] School of Mechanical Science and Engineering, Jilin University, Changchun 130025, China

mechanism and deformation mechanism deeply, which is its advantage. Therefore, theoretical modeling is more suitable for analysis in the construction phase of a machine tool.

Another modeling method is empirical modeling which maps the relationship between the thermal error and temperature variables directly and need not consider the complex heat transfer process. Compared with the theoretical modeling, empirical modeling is simpler in calculation, which is preferred in the practical application. Empirical modeling generally contains two steps: selection of the temperature-sensitivity points and choice of the error model. In order to get the data of temperatures as much as possible, a lot of temperature sensors are preliminarily installed on the parts of the machine tool. However, not all the temperatures are necessary for the error model. If there were too many inputs, the error model might have low accuracy of prediction and poor robustness due to the existence of multi-collinearity and weak anti-interference ability. Therefore, the temperature-sensitivity points as the inputs of the error model can alleviate the impact of the above problems. Selection method of temperature-sensitivity points contains correlation analysis [8], gray correlation analysis [9], fuzzy clustering [10, 11], and so on. Recently, a variety of empirical models have been studied by many scholars. The conventional methods, such as multiple regression analysis [12, 13], support vector model [14, 15], and time series model [16], and the emerging approaches including adaptive neuro-fuzzy inference system [17], sliced inverse regression (SIR) model [18], and random forest regression (RFR) modeling [19], all can construct the error model.

Usually, the temperature-sensitivity points are chosen through data clustering which is the focus of this paper. The purpose of this study is to find a more stable and effective clustering method for selection of temperature-sensitivity points in thermal error modeling.

Clustering is an important technique in data mining. Clustering is widespread in the fields of financial analysis, genomics, sensors, web documents and satellite image, etc. As for our researches, clustering plays a key role in the selection of the temperature-sensitivity points. Clustering is a process to classify the data into a number of clusters according to a specified similarity metric. In each cluster, the similarity of data is as small as possible. While in different clusters, the similarity of data is as large as possible.

Hierarchical clustering and partitional clustering are two categories of simple clustering algorithms [20]. Partitional clustering is the subject of this paper. The most popular class of partitional clustering is the center-based clustering algorithm, where KHM clustering is a representative [21].

The rest of this paper is arranged as follows: the center-based clustering algorithms are introduced, and KHM clustering is presented in Sect. 2. Section 3 introduces the cluster validity to evaluate the results of clustering, followed by evaluating the performance of the clustering algorithms through statistical experiments in Sect. 4. In Sect. 5, thermal error experiments are conducted to verify the effectiveness of the proposed clustering algorithm. Some conclusions are drawn in Sect. 6.

2 Center-based clustering algorithm

For center-based clustering algorithms [22], the computation starts with a random initialization of the center positions and follows by iterative refinement of these positions according to the memberships and weights until convergence.

2.1 A general model of center-based clustering algorithm

Define a d-dimensional data set of n points $X = \{x_1, x_2, \ldots, x_n\}$ to be clustered and a d-dimensional data set of k centers $C = \{c_1, c_2, \ldots, c_k\}$ to be iteratively updated. A membership $u(c_j/x_i)$ signifies proportion of data point x_i belonging to center c_j, where $u(c_j/x_i) \geq 0$ and $\sum_{j=k}^{k} u(c_j/x_i) = 1$. A weight function $w(x_i)$ expresses the influence of data point x_i on the recalculated center in the next iteration, where $w(x_i) > 0$.

Then, the center-based clustering algorithm can be described as a general model of iteration. The steps are shown as follows:

1. Initialize the algorithm with random centers C.
2. Classify the data according to the distances between the data and the center.
3. Calculate the value of the objective function.
4. For each data points x_i, compute its membership $u(c_j/x_i)$ and weight $w(x_i)$.
5. For each center c_j, recalculate its location according to memberships and weights of all the data points.

$$c_j = \frac{\sum_{i=1}^{n} u(c_j/x_i) w(x_i) x_i}{\sum_{i=1}^{n} u(c_j/x_i) w(x_i)} \tag{1}$$

6. Repeat steps 2–5 until convergence or reaching the maximum number of iterations

2.2 K-means clustering and fuzzy C-means clustering

These two clustering algorithms are the most favorite in the researches related to our domain. They all can be rewritten into the general form and obtain the clustering results according to the above iterative process.

K-means clustering (KM) classifies the data into k groups. For the membership function, each data point only belongs to its closest center. The objective function of KM clustering is:

$$KM(X,C)=\sum_{i}^{n}\min_{j\in\{1,2,\mathrm{L},k\}}\left\|x_i-c_j\right\|^2 \tag{2}$$

The objective function minimizes the within-cluster variance. The membership function and weight function for KM are:

$$u\left(c_j/x_i\right)=\begin{cases}1 & if\ l=\arg\min_j\left\|x_i-c_j\right\|^2\\ 0 & otherwise\end{cases}\quad w(x_i)=1 \tag{3}$$

KM clustering has a hard membership function and a constant weight function, which is easy to understand and implement.

Fuzzy C-means clustering (FCM) has a soft membership function, which allows a data point to belong partly to all the centers. The objective function of FCM clustering is:

$$FCM(X,C)=\sum_{i=1}^{n}\sum_{j=1}^{k}u_{ij}^{m}\left\|x_i-c_j\right\|^2 \tag{4}$$

where $m\geq 1$ and usually $m=2$.

The membership function and weight function of FCM are:

$$u\left(c_j/x_i\right)=\frac{\left\|x_i-c_j\right\|^{-2/(m-1)}}{\sum_{j=1}^{k}\left\|x_i-c_j\right\|^{-2/(m-1)}}\qquad w(x_i)=1 \tag{5}$$

2.3 K-harmonic means clustering

K-harmonic means clustering (KHM) is also a center-based clustering algorithm which uses the harmonic average of the distances from each data point to all the centers as its performance function. The harmonic average is defined as:

$$HA(\{a_1,\mathrm{L},a_k\})=\frac{K}{\sum_{k=1}^{K}\frac{1}{a_k}} \tag{6}$$

The objective function of KHM clustering is:

$$KHM(X,C)=\sum_{\mathrm{i}=1}^{n}\frac{k}{\sum_{j=1}^{k}\frac{1}{\left\|x_i-c_j\right\|^p}} \tag{7}$$

where p is an input parameter, and typically $p\geq 2$. The membership function and weight function for KHM are:

$$u\left(c_j/x_i\right)=\frac{\left\|x_i-c_j\right\|^{-p-2}}{\sum_{j=1}^{k}\left\|x_i-c_j\right\|^{-p-2}} \tag{8}$$

$$w(x_i)=\frac{\sum_{j=1}^{k}\left\|x_i-c_j\right\|^{-p-2}}{\left(\sum_{j=1}^{k}\left\|x_i-c_j\right\|^{-p}\right)^2} \tag{9}$$

KHM has a soft membership which makes it have a fuzzy nature. It should be noted that the weight function of KHM is varying, which is different from the above two clustering algorithms.

If there are two or more centers close to a data point, the algorithm will naturally shift one or more of these centers away to areas where the data points far away from all the centers. This will make the objective function have a lower value. On the other hand, KHM clustering assigns dynamic weight to each data point in the next iteration. This algorithm will assign a large weight to a data point which is not close to any center and a small weight to that close to one or more centers. Through dynamic weight, dense area of multiple centers can be avoided. This is the reason why KHM is insensitive to initialization.

3 Validity of clustering analysis

Clustering analysis is a kind of unsupervised calculation method, which classifies the data directly according to the characteristics of the data without prior knowledge. Almost each clustering algorithm depends on the characteristics of the dataset and its own input parameters. Inappropriate input parameters may lead to irrational results of clustering. Therefore, in order to determine the results of a clustering algorithm that fits a given dataset best, the reliable guidelines to evaluate the clustering are needed. Clustering validity indexes have been employed, which are generally defined by the combination of compactness and separability. Although there are a number of clustering validity indexes, the essence is the same, where data in each cluster is dense, and the relationships between different clusters are sparse.

There are three approaches of cluster validity: external criteria, internal criteria, and relative criteria. External criteria evaluate the results of a clustering algorithm based on a standard dataset with the known information. Internal criteria evaluate the results of a clustering algorithm using information involved in the datasets themselves. The third clustering validity, relative criteria, evaluates the results by comparing them with other clustering schemes. Internal and external validity indexes are often used in our related study.

Table 1 Descriptions of three datasets

Dataset	Breast-W		Iris			Wine		
Samples	683		150			178		
Clusters	2		3			3		
Samples of each Cluster	1	2	1	2	3	1	2	3
	444	239	50	50	50	59	71	48
Attributes	9		4			13		

3.1 External validity indexes

For the external criteria, the grouping results of the standard dataset are known in advance. Standard dataset is classified by the proposed clustering algorithm, and the obtained clustering results are compared with the known grouping results. Some common external indexes are shown as follows:

3.1.1 F-measure

F-measure of cluster j and class i is

$$F(i,j) = \frac{2Recall(i,j)\cdot Precision(i,j)}{Recall(i,j) + Precision(i,j)} \tag{10}$$

where $Recall(i, j)$ and $Precision(i, j)$ are two metrics from information retrieval, which means the recall and precision, respectively.

$$Recall(i,j) = \frac{n_{ij}}{n_i} \tag{11}$$

$$Precision(i,j) = \frac{n_{ij}}{n_j} \tag{12}$$

where n_{ij} is the number of data in class i that belongs to cluster j, n_j is the number of data in cluster j, and n_i is the number of data in class i.

To the class i, the largest value of $F(i, j)$ represents $F(i)$ value of this class, and the total F value of clustering results is

$$F = \frac{\sum_{i=1}^{c} [|i| \times F(i)]}{\sum_{i=1}^{c} |i|} \tag{13}$$

Table 2 Clustering results of Breast-W dataset

Clustering method	KM		FCM		KHM	
Cluster	1	2	1	2	1	2
1	435	18	436	22	437	26
2	9	221	8	217	7	213

Table 3 Clustering results of Iris dataset

Clustering method	KM			FCM			KHM		
Cluster	1	2	3	1	2	3	1	2	3
1	50	0	0	50	0	0	50	0	0
2	0	47	14	0	47	13	0	48	14
3	0	3	36	0	3	37	0	2	36

where $|i|$ is the number of data in class i, and c is the number of clusters. The larger value of F-measure indicates the higher clustering quality.

3.1.2 Purity and entropy

For a cluster i, p_{ij} is firstly calculated.

$$p_{ij} = \frac{n_{ij}}{n_i} \tag{14}$$

where n_{ij} is the number of objects in cluster i with class label j, n_i is the number of objects in cluster i, and the purity of cluster i is

$$P_i = \max\left(p_{ij}\right) \tag{15}$$

The overall purity of the clustering results is a weighted sum of the individual cluster purity:

$$P = \sum_{i=1}^{c} \frac{n_i}{\sum_{i=1}^{c} n_i} P_i \tag{16}$$

Entropy is very similar to purity. Entropy of cluster i is expressed as

$$E_i = -\sum_{j=1}^{c} p_{ij} \log_2\left(p_{ij}\right) \tag{17}$$

The total entropy is calculated as the weighted sum of the entropies of all clusters:

$$E = \sum_{i=1}^{c} \frac{n_i}{\sum_{i=1}^{c} n_i} E_i \tag{18}$$

Table 4 Clustering results of Wine dataset

Clustering method	KM			FCM			KHM		
Cluster	1	2	3	1	2	3	1	2	3
1	46	1	0	45	1	0	43	0	0
2	0	50	19	0	50	21	0	51	22
3	13	20	29	14	20	27	16	20	26

Table 5 Index values of clustering results for Breast-W dataset

Clustering method	F-measure	Purity	Entropy	Dunn	Iteration
KM	0.9606	0.9605	0.2401	1.7595	6
FCM	0.9654	0.9561	0.2594	1.7745	16
KHM	0.9522	0.9517	0.2770	1.7930	9

The clustering result with lower value of entropy and higher value of purity means a better clustering.

3.2 Internal validity indexes

For some experimental data without any pre-knowledge, external criteria is no longer applicable. Under this circumstance, internal criteria are an option, which evaluates the results of a clustering algorithm based on the information intrinsic to the data alone.

3.2.1 Dunn index

Dunn index is the most popular internal validity index. Dunn index is defined as:

$$Dunn = \min_{1\le i\le c}\left\{\min_{1\le j\ne i\le c}\left\{\frac{d(C_i,C_j)}{\max_{1\le k\le c}(d(C_k))}\right\}\right\} \tag{19}$$

where $d(C_i, C_j)$ defines the intercluster distance between cluster i and cluster j; $d(C_k)$ represents the intracluster distance of cluster k. The larger value of Dunn index is, the better the clustering result is.

Relevant codes of above three clustering algorithms and validity indexes are programmed by the MATLAB.

4 Statistical numerical experiment

In statistical numerical experiments, through standard datasets, the performances of clustering algorithms are tested. In this section, three famous standard datasets, Breast-W, Iris, and Wine dataset, are implemented to verify three clustering algorithms.

The first dataset is Breast-W, which is breast cancer databases obtained from the University of Wisconsin Hospitals.

Table 6 Index values of clustering results for Iris dataset

Clustering method	F-measure	Purity	Entropy	Dunn	Iteration
KM	0.8881	0.8867	0.4178	2.4437	15
FCM	0.8944	0.8933	0.3939	2.4347	43
KHM	0.8949	0.8933	0.4041	2.3999	13

Table 7 Index values of clustering results for Wine dataset

Clustering method	F-measure	Purity	Entropy	Dunn	Iteration
KM	0.6897	0.7022	0.8949	1.9032	11
FCM	0.6722	0.6854	0.9146	1.9503	57
KHM	0.6588	0.6742	0.9043	2.0981	42

This dataset has two clusters (benign and malignant) and 683 samples (samples with missing values are removed). Each sample has nine attributes about cell information. The second dataset is Iris, which is perhaps the best known database to be found in the related literatures. This dataset contains three classes of 50 instances each, where each class refers to a type of iris plant. There are four attributes, sepal length, sepal width, petal length, and petal width in a sample. The last dataset is Wine which is a chemical analysis of wines grown in the same region in Italy and derived from three different cultivars. The analysis determines the quantities of 13 constituents in each of 178 samples. Three datasets are detailed in Table 1.

Three clustering algorithms, KM, FCM, and KHM, are all employed to classify the above three datasets. The results of clustering are shown in Tables 2–4, and the validity indexes of three clustering algorithms for three datasets are calculated in Tables 5–7. A larger F-measure value, higher value of purity, lower value of entropy, and larger value of Dunn index mean a better clustering result.

For the Breast-W dataset, there are only two clusters, and the difference among the clustering results of three clustering methods is little. It can be seen in Table 2 that KM clustering is better than FCM and KHM, which requires the minimum number of iterations. The clustering result of the KHM is as

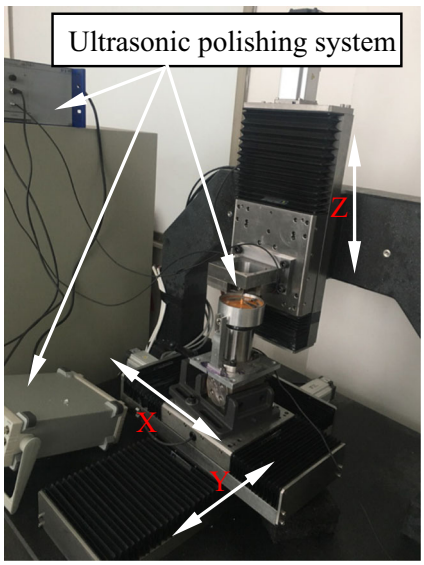

Fig. 1 Structure of the 3-axis ultrasonic polishing bench

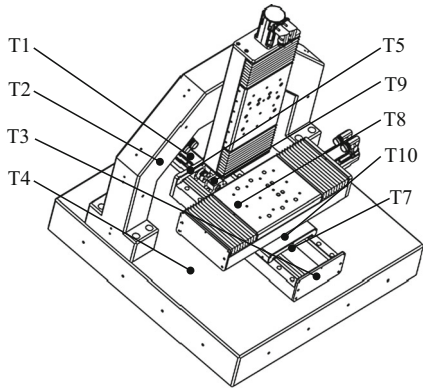

Fig. 2 Schematic diagram of the 3-axis bench and installation locations of sensors

good as that of the FCM. However, the number of iterations in KHM clustering is less.

In the Iris dataset and Wine dataset, the number of clusters becomes three and the data is crossed. As shown in Tables 3 and 4, the clustering results of three methods are almost of no difference. However, the KM cannot get the proper results every time in these two datasets. KM is sensitive to initialization. With increased number of the clusters and complexity of the data, this shortcoming is exposed. Therefore, KM may get the unreasonable results sometimes with the randomly initial cluster center, while the other two do not have such problems. Analyzing different indexes of FCM and KHM in Tables 6 and 7, KHM is better than FCM under some indexes and is worse under the other indexes. On the whole, the clustering result of two algorithms is almost the same. However, the number of iterations in KHM is less than that in FCM, which means that KHM needs less number of iterations to converge. Compared with FCM, this is the advantage of KHM.

Although the performance of KM clustering is very good with the least number of iterations, its disadvantage is obvious, which is sensitive to initialization and may lead to the improper clustering results. Ability of FCM clustering is the same as that of KHM clustering. However, with respect to number of iterations, KHM is more advantageous.

Next, the actual experiments are carried out to test the performance of KHM clustering.

5 Thermal error experiment

For the thermal error model of the machine tool, predictive accuracy and robustness were significantly affected if the multi-collinearity problem could not be solved properly. Frequently used methods give priority to reduce the multi-collinearity by grouping the temperature measurement points and selecting the temperature-sensitivity points.

Table 8 Installation locations of temperature sensors

Sensor	Location
1	Y-axis motor
2	Column
3	Front end of Y-axis guideway
4	Bed
5	Back end of Y-axis guideway
6	Environment around the machine tool
7	Front bearing of Y-axis
8	Worktable
9	Rear bearing of Y-axis
10	Leading screw nut
11	Environment of the room

The total thermal errors in a machine tool include the spindle thermal error and the feed-driving axes thermal errors. In this section, the thermal positioning error of the feed-driving axes was investigated. The temperature-sensitivity points were selected by KHM clustering. The curves of positioning error were fitted and predicted by the selected temperature-sensitivity points, and the performance of KHM clustering in the actual experiments was tested.

5.1 Experimental equipments

The experiments were conducted on a 3-axis ultrasonic polishing bench developed by our team, whose structure is exhibited in Fig. 1 and schematic diagram is shown in Fig. 2. Positioning error of *Y*-axis was taken as an example to verify the effect of KHM clustering on the actual experiments. Positioning error was measured by the laser interferometer (Renishaw XL-80), and the distribution of temperatures was detected by the temperature sensors (PT100). A total of 11 temperature sensors were preliminarily installed on the machine tool. Arrangement of the sensors is illustrated in Fig. 2. Here, T6 and T11 are not included. Installation locations of the sensors are detailed in Table 8.

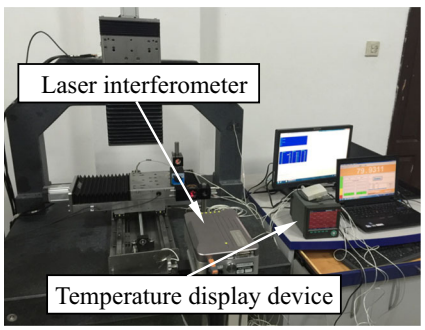

Fig. 3 Measurements of positioning error and temperatures

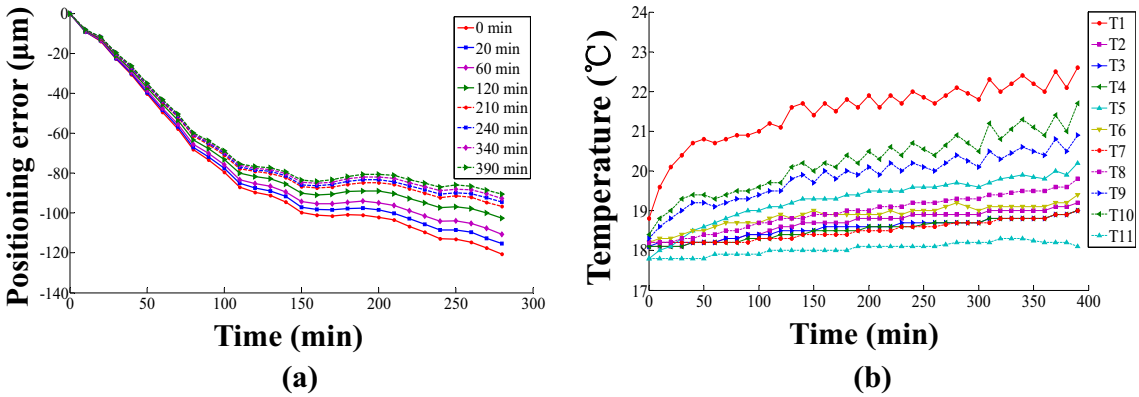

Fig. 4 Experimental data in fitting test: **a** positioning error, **b** temperatures

Table 9 *F* values of different order polynomials

Order	1	2	3	4	5	6	7	8
F value	166.59	778.50	728.74	1714.37	3488.38	3054.03	2849.25	2378.23

5.2 Measurement of experimental data

The scene of measuring the positioning error and temperatures can be seen in Fig. 3, where the ultrasonic polishing system is removed to measure the positioning error conveniently. The positioning error was bi-directionally measured every 10 mm in the stroke range of 280 mm. The geometric component of positioning error (stationary error profile) was measured when the machine tool was initially switched on (cold state). Then, the machine tool was warmed up by moving the *Y*-axis slide along its all stroke with a feed rate of 20 mm/s and an acceleration of 10 mm/s^2 until the thermal equilibrium state was reached. Positioning error was measured after the machine tool had been warmed up for 20, 50, 110, 190, 240, 340, and 390 min, respectively. Meanwhile, temperatures were synchronously measured at an interval of 10 min. The curves of positioning error and the relevant distribution of temperatures are shown in Fig. 4 (Appendix Tables 18 and 19).

Table 10 Clustering results of KHM clustering

C	Results
2	{1 9 10},{2 3 4 5 6 7 8 11}
3	{1},{5 9 10},{2 3 4 6 7 8 11}
4	{1},{9 10},{5 6 8},{2 3 4 7 11}
5	{1},{11},{5 8},{9,10},{2 3 4 6 7}
6	{1},{9},{10},{11},{5 8},{2 3 4 6 7}
7	{1},{5},{9},{10},{11},{6 8},{2 3 4 7}
8	{1},{5},{8},{9},{10},{11},{2 6},{3 4 7}
9	{1},{2},{5},{6},{8},{9},{10},{11},{3 4 7}
10	{1},{2},{3},{5},{6},{8},{9},{10},{11},{4 7}

5.3 Modeling of the positioning error

5.3.1 Fitting the geometric positioning error

Due to the polynomial with explicit expression and simple calculation, polynomial fitting is the most common modeling method for the geometric error terms of machine tools. For the geometric error of each axis, the value is zero at its zero position [23]. As a result, the constant term of the polynomial should be neglected, and one *n*th-order polynomial without the constant term is described as:

$$\delta_{pp}(P) = \sum_{i=1}^{n} \alpha_i p^i \tag{20}$$

where p is the nominal coordinate of P-axis. By expanding and transforming Eq. (20), the following equation can be obtained.

$$X\beta = y \tag{21}$$

where $X = \begin{bmatrix} p_1 & p_1^2 & \cdots & p_1^n \\ p_2 & p_2^2 & \cdots & p_2^n \\ \vdots & \vdots & \cdots & \vdots \\ p_m & p_m^2 & \cdots & p_m^n \end{bmatrix}$; n is the order of the polynomial; m is the number of the measurement points; β are the coefficients, and $\beta = [\alpha_1, \alpha_2, \cdots, \alpha_n]^T$; y are geometric errors (positioning errors in this paper), and $y = [\delta_{pp}(p_1), \delta_{pp}(p_2), \cdots, \delta_{pp}(p_m)]^T$.

Equation (21) can be solved through least square (LS) to obtain the coefficients, which can be written as follows:

$$\beta = \left(X^T X\right)^{-1} X^T y \tag{22}$$

Then, there is need to seek the appropriate order of the polynomial. According to the reference [24], the polynomial

Table 11 Index value of each clustering result

C	2	3	4	5	6	7	8	9	10
Dunn	2.8840	3.5749	2.9663	2.7264	2.2553	3.4227	2.3010	4.2408	2.4433

models are evaluated by F test to choose the best order of the polynomial. F value of the nth-order polynomial is:

$$F(n) = \frac{\frac{1}{n}\sum_{i=1}^{m}\left(y_n(p_i)-\overline{y}\right)^2}{\frac{1}{m-n-1}\sum_{i=1}^{m}\left(y_i-y_n(p_i)\right)^2} \tag{23}$$

where, y_i is the measured value; $\overline{y}$ represents the mean value of measured data; $y_n(p_i)$ means the output value of nth-order polynomial.

A series of polynomials from first-order to eighth-order are obtained using the Eq. (22), where $y(i)$ represents the ith-order polynomial, and x is the nominal coordinate. The F values of these eight polynomials are calculated in Table 9.

$$\begin{cases} y(1) = -0.5237x \\ y(2) = -0.9334x + 0.0019x^2 \\ y(3) = -1.0881x + 0.0037x^2 - 4.7713 \times 10^{-6}x^3 \\ y(4) = -0.7700x - 0.0030x^2 + 3.6498 \times 10^{-5}x^3 - 7.7347 \times 10^{-8}x^4 \\ y(5) = -0.4812x - 0.0125x^2 + 1.3657 \times 10^{-4}x^3 - 4.9980 \times 10^{-7}x^4 + 6.1912 \times 10^{-10}x^5 \\ y(6) = -0.5878x - 0.0075x^2 + 5.7231 \times 10^{-5}x^3 + 5.9050 \times 10^{-8}x^4 - 1.1848 \times 10^{-9}x^5 \\ \quad + 2.1778 \times 10^{-12}x^6 \\ y(7) = -0.7582x + 0.0033x^2 - 1.8081 \times 10^{-4}x^3 + 2.5208 \times 10^{-6}x^4 - 1.4204 \times 10^{-8}x^5 \\ \quad + 3.6275 \times 10^{-11}x^6 - 3.5061 \times 10^{-14}x^7 \\ y(8) = -0.7350x + 0.0014x^2 - 1.2548 \times 10^{-4}x^3 + 1.7399 \times 10^{-6}x^4 - 8.2322 \times 10^{-9}x^5 \\ \quad + 1.0980 \times 10^{-11}x^6 + 2.0747 \times 10^{-14}x^7 - 5.0033 \times 10^{-17}x^8 \end{cases} \tag{24}$$

The larger the F value is, the better the polynomial is. The maximum F value is 3488.38, which means that fifth-order polynomial is chosen as the model of geometric positioning error, and it is rewritten the following formation:

$$\begin{aligned} \delta_{yy}(Y) = {} & -0.4812y - 0.0125y^2 + 1.3657 \\ & \times 10^{-4}y^3 - 4.9980 \times 10^{-7}y^4 + 6.1912 \\ & \times 10^{-10}y^5 \end{aligned} \tag{25}$$

Table 12 Thermal-variant slopes

No.	Curve slope
0	− 0.39521
1	− 0.37671
2	− 0.35904
3	− 0.33037
4	− 0.30924
5	− 0.30191
6	− 0.29493
7	− 0.28767

5.3.2 Selection of the temperature-sensitivity points

KHM clustering is applied to classify the temperature variables, and each group selects one representative variable. Then, these representative variables establish the thermal error model.

There are totally 11 temperature sensors in the experiments, which could obtain 11 different classification results. While,

Table 13 Values and sorting of correlation coefficients

Temperature variable	Value	Sorting
T1	0.9725	2
T2	0.9660	5
T3	0.9538	6
T4	0.9160	9
T5	0.9814	1
T6	0.9673	3
T7	0.8536	11
T8	0.9382	8
T9	0.9667	4
T10	0.9440	7
T11	0.8889	10

Table 14 Model summary of two models

Model	R	R square	Adjusted R square	Std. error of the estimate
I	0.994	0.987	0.978	0.006031386
II	1.000	1.000	1.000	0.000262071

all in one group and each one in a group are meaningless, which are not considered. Clustering results by KHM clustering are shown in Table 10, where C is number of clusters.

There is not any pre-knowledge about the temperature data. Therefore, internal validity index, Dunn index, evaluates the clustering results. The index value of each clustering result is computed in Table 11. Through analysis of the Dunn validity index, the best clustering result corresponds to the maximum value of the validity index. The maximum value is 4.2408, which divides the temperature data into nine groups. While, the second largest value is 3.5749, which classifies the temperature data into three clusters. The number of clusters indicates the number of variables in the final error model. The less variables the model contains, the simpler it is. Therefore, the model containing three variables is simpler than that of nine variables, which is more effective in practical application. Actually, nine variables in the error model are too much, which is not appropriate for error modeling. If the difference between the precision of two models is little, the model of three variables will be selected.

Each group selects one representative variable which has the highest correlation coefficient with respect to the thermal-variant slopes of the thermal positioning error. The thermal-variant slopes are got by fitting the curves of thermal positioning error with first-order polynomial in Fig. 4a, which is shown in Table 12. Correlation coefficient between x_i and x_j is calculated as follows:

$$r_{ij} = \frac{\sum_{k=1}^{m}\left(x_{ik}-\overline{x_i}\right)\left(x_{jk}-\overline{x_j}\right)}{\sqrt{\sum_{k=1}^{m}\left(x_{ik}-\overline{x_i}\right)^2}\sqrt{\sum_{k=1}^{m}\left(x_{jk}-\overline{x_j}\right)^2}} \quad (26)$$

Then, the correlation coefficients between the temperature variables and the thermal-variant coefficients are shown in Table 13.

Table 15 Variance analysis of two models

Model		Sum of squares	df	Mean square	F	Sig.
I	Regression	0.011	3	0.004	103.960	0.000
	Residual	0.000	4	0.000		
	Total	0.011	7			
II	Regression	0.011	6	0.002	27,884.625	0.005
	Residual	0.000	1	0.000		
	Total	0.011	7			

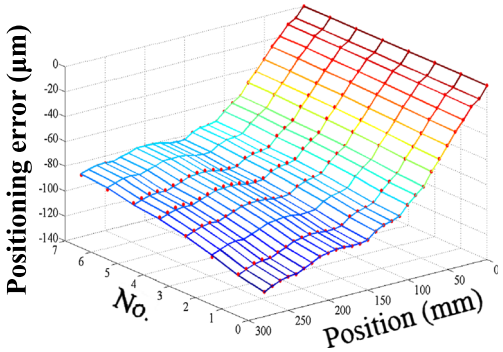

Fig. 5 Fitting results of MLR-KHM model

According to correlation coefficients and clustering results, T_1, T_2, T_3, T_5, T_6, T_8, T_9, T_{10}, and T_{11} are selected as the representative temperature variables of the error model with nine variables, and the representative temperature variables T_1, T_5, and T_6 are regarded as the inputs of the error model of three variables.

The simpler the error model is, the more effective it is applied. The purpose of this study is to validate the effectiveness of KHM clustering on selection of temperature-sensitivity points in the thermal error modeling. Due to multiple linear regression having a simple structure and low computational complexity, multiple linear regression combined with KHM clustering is adopted to construct the thermal error model, which is called MLR-KHM model.

Through analyzing the results of two multiple linear regression models, the model which is more suitable for error modeling is selected. The thermal error model of three variables is:

$$k_i = -0.00182T_1 + 0.07734T_5 - 0.05795T_6 - 0.68157 \quad (27)$$

However, when the number of variables is 9, the tolerance is exceeded, and three variables have to be excluded. The thermal error model is:

$$k_i' = 0.01507T_1 + 0.09951T_2 - 0.03639T_3 + 0.02568T_6 - 0.03965T_8 + 0.02082T_{11} - 1.93720 \quad (28)$$

The analysis results of two error models are given in Table 14 and Table 15, where Model I represents the model with three variables, and Model II is the other model. It can be seen that there is little difference between the sample determination coefficients of two models, and the regression equation of Model I is more significant than that of Model II. Precision of Model I is almost not reduced comparing with Model II,

Table 16 Evaluation criteria of fitting test

Criterion	RSME	R^2	η
Fitting test	0.7005	0.9995	99.25%

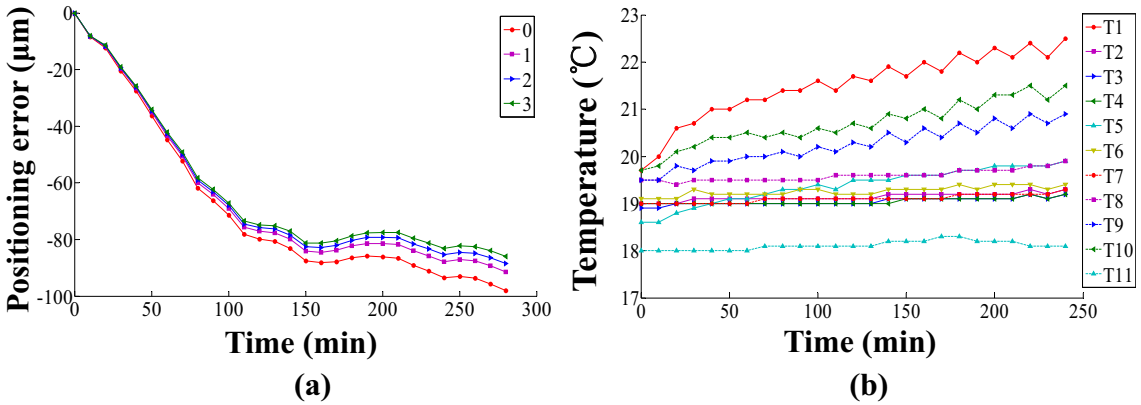

Fig. 6 Experimental data in verification test: **a** positioning error, **b** temperatures

and it only has three variables. Therefore, Model I is better. Finally, T_1, T_5, and T_6 are regarded as the inputs of the error model.

5.3.3 Modeling of the comprehensive positioning error

Error model is as simple as possible. The relationship between the thermal-variant slopes and three representative temperature variables is mapped by MLR-KHM model, which is shown as Eq. (27) .

The geometric component and thermal component are put together to form the comprehensive positioning error [25–27], which can be expressed as:

$$\delta_{yy}(Y,T) = \delta_{yy}(Y) + \delta_{yy}(T) \tag{29}$$

$$\delta_{yy}(T) = (k_i - k_0)y \tag{30}$$

where $\delta_{yy}(Y,T)$ is comprehensive positioning error; $\delta_{yy}(Y)$ is the geometric component of positioning error; $\delta_{yy}(T)$ is the thermal term of positioning error; k_0 is the slope of the geometric positioning error curve; k_i is the slope of ith thermal positioning error curve.

Equation (25) and Eq. (27) are substituted into Eq. (29) and Eq. (30), and the comprehensive positioning error is obtained.

$$\begin{aligned}\delta_{yy}(Y,T) &= -0.4812y - 0.0125y^2 + 1.3657\times10^{-4}y^3 - 4.9980\times10^{-7}y^4 + 6.1912\times10^{-10}y^5 \\ &\quad + (-0.00182T_1 + 0.07734T_5 - 0.05795T_6 - 0.68157 + 0.39521)y \\ &= (-0.00182T_1 + 0.07734T_5 - 0.05795T_6 - 0.76756)y - 0.0125y^2 + 1.3657\times10^{-4}y^3 \\ &\quad - 4.9980\times10^{-7}y^4 + 6.1912\times10^{-10}y^5\end{aligned} \tag{31}$$

Fitting results with Eq. (31) are exhibited in Fig. 5, where the curves from 0 to 7 represent the positioning errors from 0 min to 390 min successively, and the measured data is marked with dots.

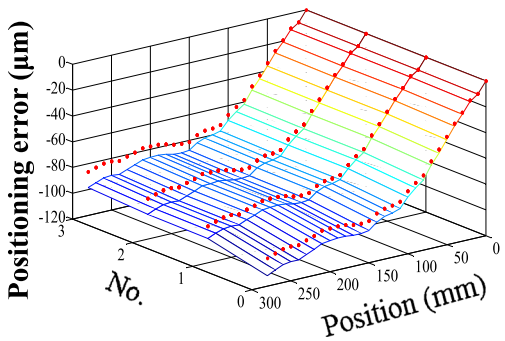

Fig. 7 Prediction results of MLR-KHM model

Then, the proposed error models' goodness of fitting is quantitatively evaluated. Three evaluation criteria, RMSE (root mean squared error), R^2 (coefficient of determination), and η (predicting accuracy) are presented.

$$RSME = \sqrt{\frac{1}{n}\sum_{i=1}^{n}(x_i - \hat{x}_i)^2} \tag{32}$$

$$R^2 = 1 - \frac{\sum_{i=1}^{n}(x_i - \hat{x}_i)^2}{\sum_{i=1}^{n}\left(x_i - \overline{x}\right)^2} \tag{33}$$

$$\eta = 1 - \frac{\sum_{i=1}^{n}|x_i - \hat{x}_i|}{\sum_{i=1}^{n}|x_i|} \times 100\% \tag{34}$$

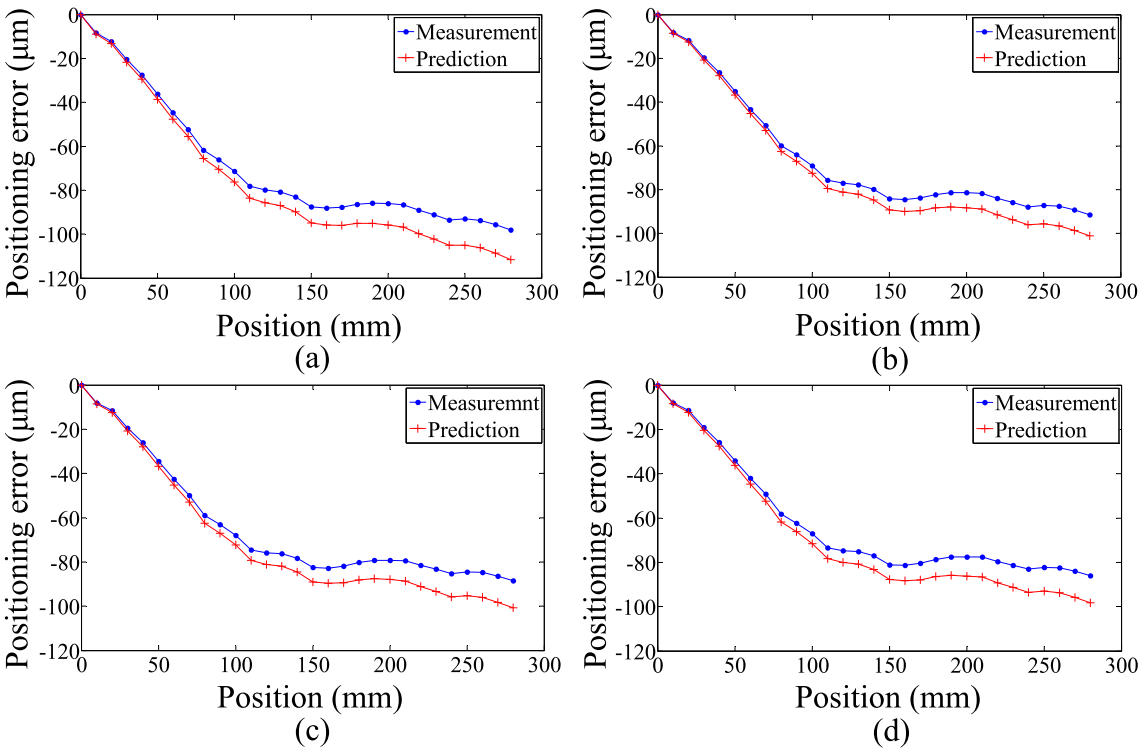

Fig. 8 Prediction result of each curve: **a** prediction result of curve 0, **b** prediction result of curve 1, **c** prediction result of curve 2, **d** prediction result of curve 3

where x_i is the measured value, $\hat{x}_i$ is the output value of error model, and $\bar{x} = \sum_{i=1}^{n} x_i$ is the mean of the measured values. The values of three evaluation criteria are calculated in Table 16.

5.3.4 Predictive performance of the error model

To verify the predictive ability and robustness of MLR-KHM model, another experiment was conducted. The machine tool was warmed up by moving the *Y*-axis slide with a feed rate of 15 mm/s and an acceleration of 8 mm/s^2.

The positioning errors, after machine tool had been warmed up for 50, 120, 140, and 220 min, were measured. At the same time, temperature data was recorded. The curves of positioning error are shown in Fig. 6a, which are represented by the number 0, 1, 2, and 3, respectively. The corresponding temperature curves are depicted in Fig. 6b (Appendix Tables 20 and 21).

The above positioning errors were predicted by the MLR-KHM model. The prediction results are shown in Fig. 7 (the measured data marked with dots). In order to depict more clearly, each predicted and measured curves of positioning error are described in Fig. 8. Model evaluations are calculated in Table 17.

In general, thermal error models could achieve an excellent fitting accuracy. However, predictive deviations will enlarge usually under other operating conditions. This is due to changes of machine tool thermal state under different operating states. An excellent error model does not only have high fitting precision but also strong robustness, which can maintain high accuracy of prediction even under different operating conditions.

In Fig. 5 and Fig. 7, it can be found that the differences between the measured values and predictive values of the verification test become larger comparing with the differences between the measured values and fitting values of fitting test. Through comparing the values of the three evaluation criteria in Tables 16 and 17, performance of MLR-KHM model in fitting is better than that in prediction. Although the predictive accuracy of the proposed error model decreases somewhat, it is good enough for the error compensation. It is proved that MLR-KHM model has strong robustness, which can meet the requirements of error compensation. Therefore, KHM clustering is a reliable method to select temperature-sensitivity points, and MLR-KHM model is an alternative method to construct the thermal error.

Table 17 Evaluation criteria of verification test

Criterion	RSME	R^2	η
Verification test	6.9690	0.9356	90.86%

6 Conclusions

The key of this paper is to propose a clustering method, KHM clustering, which is used for the first time in the field of thermal error modeling. The following conclusions can be drawn:

1. Through statistical numerical experiments, KHM clustering is more stable and insensitive to initialization comparing with the KM clustering. KM clustering sometimes gets the unreasonable results, while the KHM clustering does not. Although the results obtained by the KHM clustering and FCM clustering are almost the same, the number of iterations in the convergence of KHM clustering is less than that of FCM clustering. These are the advantages of KHM clustering.
2. In the actual experiments, the temperature-sensitivity points are selected by the KHM clustering. KHM clustering with the help of Dunn validity index selects three temperature-sensitivity points from 11 temperature points to build the thermal error model. Effectiveness of MLR model combined with KHM clustering is verified. Therefore, MLR-KHM model can be a candidate method of thermal error modeling.
3. The effect of MLR-KHM thermal error model proposed in this article is only verified when the machine tool is in an idle state. For the actual cutting state, the thermal error model still needs further research.

Funding information This work is supported by the National Key Basic Research and Development Program (973 Program) of China (grant no. 2011CB706702), Natural Science Foundation of China (grant no. 51135006 and 51305161), Jilin province science and technology development plan item (grant no. 20130101042JC), and Project 2017140 supported by Graduate Innovation Fund of Jilin University (grant no. 2017140).

Appendix

Table 18 Positioning error of fitting test

No. Position	0	1	2	3	4	5	6	7
0	0	0	0	0	0	0	0	0
10	− 9.2	− 9.1	− 8.9	− 8.6	− 8.3	− 8.3	− 8.2	− 8.1
20	− 13.9	− 13.6	− 13.2	− 12.7	− 12.3	− 12	− 11.9	− 11.8
30	− 22.8	− 22.4	− 21.8	− 21.1	− 20.4	− 20.1	− 19.9	− 19.7
40	− 30.7	− 30	− 29.3	− 28.1	− 27.3	− 27.1	− 26.6	− 26.3
50	− 40.3	− 39.6	− 38.6	− 37.2	− 36.1	− 35.8	− 35.4	− 35
60	− 49.5	− 48.4	− 47.4	− 45.6	− 44.4	− 43.9	− 43.5	− 43.1
70	− 57.9	− 56.7	− 55.4	− 53.4	− 51.9	− 51.4	− 50.9	− 50.4
80	− 68.2	− 67.1	− 65.5	− 63.3	− 61.3	− 60.6	− 60.4	− 59.8
90	− 73.4	− 71.8	− 70.2	− 67.6	− 65.7	− 65	− 64.4	− 63.8
100	− 79.5	− 77.5	− 75.9	− 73.1	− 70.9	− 70	− 69.5	− 68.7
110	− 87.1	− 85.1	− 83.2	− 80	− 77.7	− 76.9	− 76.1	− 75.3
120	− 89.6	− 87.5	− 85.2	− 81.8	− 79.2	− 78.5	− 77.5	− 76.7
130	− 91.2	− 88.9	− 86.6	− 82.8	− 80.1	− 79.1	− 78.2	− 77.3
140	− 94.4	− 91.6	− 89.4	− 85.5	− 82.2	− 81.4	− 80.3	− 79.3
150	− 99.7	− 97	− 94.3	− 90.1	− 86.8	− 85.8	− 84.7	− 83.6
160	− 101.1	− 98.3	− 95.4	− 90.9	− 87.4	− 86.3	− 85.1	− 84.1
170	− 101.5	− 98.5	− 95.4	− 90.6	− 86.9	− 85.7	− 84.5	− 83.3
180	− 100.9	− 97.7	− 94.6	− 89.3	− 85.6	− 84.2	− 82.8	− 81.7
190	− 101.1	− 97.5	− 94.1	− 88.9	− 84.8	− 83.3	− 82	− 80.6
200	− 102.2	− 98.5	− 94.8	− 89	− 84.8	− 83.3	− 82	− 80.6
210	− 103.5	− 100.2	− 96.2	− 90.2	− 85.7	− 84.3	− 82.6	− 81.1

Table 18 (continued)

No. Position	0	1	2	3	4	5	6	7
220	− 106.8	− 102.9	− 98.9	− 92.7	− 87.9	− 86.4	− 84.8	− 83.2
230	− 109.7	− 105.6	− 101.5	− 94.9	− 90	− 88.3	− 86.7	− 85.1
240	− 112.8	− 108.5	− 104.2	− 97.4	− 92.2	− 90.5	− 88.8	− 87.1
250	− 113.1	− 108.5	− 104	− 96.8	− 91.5	− 89.8	− 88.1	− 86
260	− 114.6	− 109.6	− 105.2	− 97.8	− 92	− 90.2	− 88.4	− 86.5
270	− 117.4	− 112.7	− 107.6	− 100	− 94.6	− 92.2	− 90.3	− 88.5
280	− 120.6	− 115.3	− 110.7	− 102.5	− 96.6	− 94.5	− 92.7	− 90.6

Table 19 Temperature of fitting test

Point Time	T_1	T_2	T_3	T_4	T_5	T_6	T_7	T_8	T_9	T_{10}	T_{11}
0	18.8	18.1	18.1	18.1	17.8	18.2	18.2	18.2	18.3	18.4	17.8
10	19.6	18.1	18.2	18.1	18	18.3	18.2	18.2	18.6	18.8	17.8
20	20.1	18.1	18.2	18.1	18.1	18.3	18.2	18.2	18.8	19	17.8
30	20.4	18.1	18.2	18.1	18.3	18.4	18.2	18.3	19	19.3	17.8
40	20.7	18.2	18.2	18.2	18.5	18.5	18.2	18.3	19.2	19.4	17.8
50	20.8	18.2	18.2	18.2	18.6	18.5	18.2	18.4	19.2	19.4	17.8
60	20.7	18.2	18.2	18.2	18.7	18.6	18.2	18.4	19.1	19.3	17.9
70	20.8	18.3	18.3	18.2	18.8	18.7	18.2	18.5	19.2	19.4	17.9
80	20.9	18.3	18.3	18.2	18.9	18.7	18.2	18.5	19.3	19.5	17.9
90	20.9	18.4	18.4	18.3	19	18.7	18.2	18.6	19.3	19.5	17.9
100	21	18.4	18.4	18.3	19	18.7	18.3	18.7	19.4	19.6	17.9
110	21.2	18.5	18.4	18.3	19.1	18.8	18.3	18.7	19.5	19.7	18
120	21.1	18.6	18.5	18.4	19.1	18.9	18.3	18.8	19.5	19.7	18
130	21.6	18.6	18.5	18.4	19.2	18.8	18.3	18.8	19.8	20.1	18
140	21.7	18.7	18.5	18.4	19.3	18.9	18.4	18.8	19.9	20.2	18
150	21.4	18.7	18.5	18.5	19.3	19	18.4	18.9	19.7	20	18
160	21.7	18.7	18.6	18.5	19.3	18.9	18.4	18.9	20	20.2	18
170	21.5	18.7	18.6	18.5	19.3	18.9	18.4	18.9	19.8	20.1	18
180	21.8	18.7	18.6	18.5	19.4	18.9	18.4	19	20	20.4	18
190	21.6	18.8	18.6	18.5	19.4	18.9	18.5	19	19.9	20.2	18.1
200	21.9	18.8	18.6	18.6	19.5	18.9	18.5	19	20.1	20.5	18.1
210	21.6	18.8	18.6	18.6	19.5	18.9	18.5	19.1	19.9	20.3	18.1
220	21.9	18.8	18.6	18.6	19.5	19	18.5	19.1	20.2	20.6	18.1
230	21.7	18.8	18.7	18.6	19.5	18.9	18.6	19.1	20	20.4	18.1
240	22	18.9	18.7	18.6	19.6	19	18.6	19.2	20.2	20.7	18.1
250	21.85	18.9	18.7	18.65	19.6	19	18.6	19.2	20.1	20.55	18.1
260	21.7	18.9	18.7	18.7	19.6	19	18.6	19.2	20	20.4	18.1
270	21.9	18.9	18.7	18.7	19.65	19.1	18.65	19.25	20.2	20.65	18.15
280	22.1	18.9	18.7	18.7	19.7	19.2	18.7	19.3	20.4	20.9	18.2
290	21.95	18.9	18.7	18.7	19.65	19.1	18.7	19.3	20.25	20.7	18.2
300	21.8	18.9	18.7	18.7	19.6	19	18.7	19.3	20.1	20.5	18.2
310	22.3	19	18.8	18.8	19.7	19.1	18.7	19.4	20.5	21.2	18.2
320	22	19	18.8	18.8	19.8	19.1	18.8	19.4	20.3	20.8	18.3

Table 19 (continued)

Point Time	T_1	T_2	T_3	T_4	T_5	T_6	T_7	T_8	T_9	T_{10}	T_{11}
330	22.2	19	18.8	18.8	19.85	19.1	18.8	19.45	20.45	21.05	18.3
340	22.4	19	18.8	18.8	19.9	19.1	18.8	19.5	20.6	21.3	18.3
350	22.2	19	18.8	18.8	19.85	19.1	18.8	19.5	20.5	21.1	18.25
360	22	19	18.8	18.8	19.8	19.1	18.8	19.5	20.4	20.9	18.2
370	22.5	19.1	18.9	18.9	20	19.2	18.9	19.6	20.8	21.4	18.2
380	22.1	19.1	18.9	18.9	19.9	19.2	18.9	19.6	20.5	21	18.2
390	22.6	19.2	19	19	20.2	19.4	19	19.8	20.9	21.7	18.1

Table 20 Positioning error of verification test

No. Position	0	1	2	3
0	0	0	0	0
10	− 8.4	− 8.2	− 8.1	− 8
20	− 12.3	− 11.8	− 11.6	− 11.4
30	− 20.4	− 19.7	− 19.4	− 19.1
40	− 27.5	− 26.5	− 26.1	− 25.8
50	− 36.3	− 35.1	− 34.6	− 34.1
60	− 44.7	− 43.3	− 42.6	− 42.1
70	− 52.3	− 50.6	− 49.9	− 49.2
80	− 61.8	− 59.9	− 59	− 58.3
90	− 66.2	− 64	− 63.1	− 62.3
100	− 71.4	− 69.1	− 68	− 67.1
110	− 78.2	− 75.7	− 74.5	− 73.5
120	− 79.9	− 77.1	− 75.8	− 74.8
130	− 80.7	− 77.7	− 76.3	− 75.1
140	− 83.1	− 79.9	− 78.4	− 77.1
150	− 87.6	− 84.1	− 82.5	− 81.2
160	− 88.2	− 84.5	− 82.8	− 81.3
170	− 87.8	− 83.8	− 82	− 80.5
180	− 86.4	− 82.2	− 80.3	− 78.7
190	− 85.8	− 81.4	− 79.3	− 77.6
200	− 86.1	− 81.4	− 79.3	− 77.5
210	− 86.6	− 81.7	− 79.4	− 77.5
220	− 89.1	− 83.9	− 81.6	− 79.6
230	− 91.2	− 85.8	− 83.3	− 81.3
240	− 93.5	− 87.9	− 85.3	− 83.1
250	− 93	− 87.1	− 84.5	− 82.2
260	− 93.7	− 87.6	− 84.8	− 82.5
270	− 95.7	− 89.3	− 86.5	− 84
280	− 98.1	− 91.5	− 88.5	− 86

Table 21 Temperature of verification test

Point Time	T_1	T_2	T_3	T_4	T_5	T_6	T_7	T_8	T_9	T_{10}	T_{11}
0	19.7	19	18.9	19	18.6	19.1	19	19.5	19.5	19.7	18
10	20	19	18.9	19	18.6	19.1	19	19.5	19.5	19.8	18
20	20.6	19	19	19	18.8	19.1	19	19.4	19.8	20.1	18
30	20.7	19.1	19	19	18.9	19.3	19	19.5	19.7	20.2	18
40	21	19.1	19	19	19	19.2	19	19.5	19.9	20.4	18
50	21	19.1	19	19	19.1	19.2	19	19.5	19.9	20.4	18
60	21.2	19.1	19	19	19.1	19.2	19	19.5	20	20.5	18
70	21.2	19.1	19	19	19.2	19.2	19.1	19.5	20	20.4	18.1
80	21.4	19.1	19	19	19.3	19.2	19.1	19.5	20.1	20.5	18.1
90	21.4	19.1	19	19	19.3	19.3	19.1	19.5	20	20.4	18.1
100	21.6	19.1	19	19	19.4	19.3	19.1	19.5	20.2	20.6	18.1
110	21.4	19.1	19	19	19.3	19.2	19.1	19.6	20.1	20.5	18.1
120	21.7	19.1	19	19	19.5	19.2	19.1	19.6	20.3	20.7	18.1
130	21.6	19.1	19	19	19.5	19.2	19.1	19.6	20.2	20.6	18.1
140	21.9	19.2	19.1	19	19.5	19.3	19.1	19.6	20.5	20.9	18.2
150	21.7	19.2	19.1	19.1	19.6	19.3	19.1	19.6	20.3	20.8	18.2
160	22	19.2	19.1	19.1	19.6	19.3	19.1	19.6	20.6	21	18.2
170	21.8	19.2	19.1	19.1	19.6	19.3	19.1	19.6	20.4	20.8	18.3
180	22.2	19.2	19.1	19.1	19.7	19.4	19.2	19.7	20.7	21.2	18.3
190	22	19.2	19.1	19.1	19.7	19.3	19.2	19.7	20.5	21	18.2
200	22.3	19.2	19.1	19.1	19.8	19.4	19.2	19.7	20.8	21.3	18.2
210	22.1	19.2	19.1	19.1	19.8	19.4	19.2	19.7	20.6	21.3	18.2
220	22.4	19.3	19.2	19.2	19.8	19.4	19.2	19.8	20.9	21.5	18.1
230	22.1	19.2	19.1	19.1	19.8	19.3	19.2	19.8	20.7	21.2	18.1
240	22.5	19.3	19.2	19.2	19.9	19.4	19.3	19.9	20.9	21.5	18.1

References

1. Bryan JB (1990) International status of thermal error research. CIRP Ann-Manuf Technol 39(2):645–656
2. Ni J (1997) CNC machine accuracy enhancement through real-time error compensation. J Manuf Sci Eng Trans ASME 119:717–725
3. Li Y, Zhao WH, Lan SH, Ni J, Wu WW, Lu BH (2015) A review on spindle thermal error compensation in machine tools. Int J Mach Tools Manuf 95:20–38
4. Mian NS, Fletcher S, Longstaff AP, Myers A (2013) Efficient estimation by FEA of machine tool distortion due to environmental temperature perturbations. Precis Eng 37:372–379
5. Yang J, Zhang DS, Mei XS, Zhao L, Ma C, Shi H (2014) Thermal error simulation and compensation in a jig-boring machine equipped with a dual-drive servo feed system. Proc IMechE, Part B: J Eng Manuf 229(1 Suppl):43–63
6. Ma C, Mei XS, Yang J, Zhao L, Shi H (2015) Thermal characteristics analysis and experimental study on the high-speed spindle system. Int J Adv Manuf Technol 79(1–4):469–489
7. Fan KG (2016) Research on the machine tool's temperature spectrum and its application in a gear form grinding machine. Int J Adv Manuf Technol 90(9–12):3841–3850
8. Guo QJ, Yang JG, Wu H (2010) Application of ACO-BPN to thermal error modeling of NC machine tool. Int J Adv Manuf Technol 50:667–675
9. Yan JY, Yang JG (2008) Application of synthetic grey correlation theory on thermal point optimization for machine tool thermal error compensation. Int J Adv Manuf Technol 43(11–12):1124–1132
10. Han J, Wang LP, Wang HT, Cheng NB (2011) A new thermal error modeling method for CNC machine tools. Int J Adv Manuf Technol 62(1–4):205–212
11. Wang HT, Wang LP, Li TM, Han J (2013) Thermal sensor selection for the thermal error modeling of machine tool based on the fuzzy clustering method. Int J Adv Manuf Technol 69(1–4):121–126
12. Chen JS, Yuan J, Ni J (1996) Thermal error modeling for real-time error compensation. Int J Adv Manuf Technol 12(4):266–275
13. Wu CW, Tang CH, Chang CF, Shiao YS (2011) Thermal error compensation method for machine center. Int J Adv Manuf Technol 59(5–8):681–689
14. Ramesh R, Mannan MA, Poo AN (2002) Support vector machines model for classification of thermal error in machine tools. Int J Adv Manuf Technol 20(2):114–120
15. Miao EM, Gong YY, Niu PC, Ji CZ, Chen HD (2013) Robustness of thermal error compensation modeling models of CNC machine tools. Int J Adv Manuf Technol 69(9–12):2593–2603

16. Yang J, Zhang DS, Feng B, Mei XS, Hu ZB (2014) Thermal-induced errors prediction and compensation for a coordinate boring machine based on time series analysis. Math Probl Eng 2014:1–13. https://doi.org/10.1155/2014/784218
17. Dai H, Wang S, Xiong X (2017) Thermal error modelling of motorised spindle in large-sized gear grinding machine. Proc IMechE, Part B: J Eng Manuf 231(5):768–778
18. Zhang T, Ye WH, Shan YC (2016) Application of sliced inverse regression with fuzzy clustering for thermal error modeling of CNC machine tool. Int J Adv Manuf Technol 85(9):1–11
19. Lei MH, Jiang GD, Yang J, Mei XS, Xia P, Zhao L (2017) Thermal error modeling with dirty and small training sample for the motorized spindle of a precision boring machine. Int J Adv Manuf Technol 2017(2):1–16
20. Güngör Z, Ünler A (2008) K-harmonic means data clustering with tabu-search method. Appl Math Model 32(6):1115–1125
21. Zhang B, Hsu M, Dayal U (1999) K-Harmonic Means- A Data Clustering Algorithm
22. Hamerly G, Elkan C (2002) Alternatives to the k-means algorithm that find better clusterings. Eleventh International Conference on Information and Knowledge Management. ACM 2002:600–607
23. Wu CJ, Fan JW, Wang QH, Pan R, Tang YH, Li ZS (2017) Prediction and compensation of geometric error for translational axes in multi-axis machine tools. Int J Adv Manuf Tech 9–12:1–23
24. Fu GQ, Zhang L, Fu JZ, Gao HL, Jin YA (2017) *F* test-based automatic modeling of single geometric error component for error compensation of five-axis machine tools. Int J Adv Manuf Tech 2:1–13
25. Li ZH, Fan KG, Yang JG, Zhang Y (2014) Time-varying positioning error modeling and compensation for ball screw systems based on simulation and experimental analysis. Int J Adv Manuf Technol 73(5–8):773–782
26. Jiang H, Fan KG, Yang JG (2014) An improved method for thermally induced positioning errors measurement, modeling, and compensation. Int J Adv Manuf Technol 75(9–12):1279–1289
27. Li ZH, Yang JG, Fan KG, Zhang Y (2015) Integrated geometric and thermal error modeling and compensation for vertical machining centers. Int J Adv Manuf Tech 76(5):1139–1150